J. Fluid Mech. (1992), *vol.* 237, *pp.* 1–11
Printed in Great Britain

Dynamics and transport of a localized soluble surfactant on a thin film

By D. HALPERN AND J. B. GROTBERG

Biomedical Engineering Department, Robert R. McCormick School of Engineering and Applied Science, Northwestern University, Evanston, IL 60208, USA *and* Department of Anesthesia, Northwestern University Medical School, Chicago, IL 60611, USA

(Received 20 August 1990 and in revised form 17 January 1991)

The flow induced by a localized droplet of soluble surfactant on the surface of a thin film is analysed, motivated by an interest in the interaction between inhaled droplets and the lung's thin liquid lining after an aerosol lands on its surface. The spreading is driven by gradients of surface tension and results in flow of the droplet and underlying liquid film. This induced flow field plays an important role in the transport of dissolved species from the droplet, through the film, and to the tissue for absorption.

Evolution equations for the film thickness, surface and bulk liquid concentrations are derived using lubrication theory, since the depth of the film is much smaller than the characteristic radius of the droplet. Solutions are obtained numerically using the method of lines for a variety of surface Péclet numbers.

We find that the effect of solubility is to decrease both film disturbances and surface concentrations, and to induce an absorption-driven backflow. In addition, there is a gravity-driven backflow from hydrostatics. At large surface Péclet numbers, large film disturbances are obtained and more surfactant is able to diffuse across the rigid permeable wall, while surface diffusion causes more rapid spreading and decreases film disturbances. Gravity acts as a restoring force by creating a bi-directional flow, and hence disenhances the vertical flux of surfactant across the air–liquid interface. This model may have implications for the delivery of drugs by aerosol inhalation.

1. Introduction

The aim of this paper is to develop a theoretical model for the flow induced by a localized droplet of soluble surfactant on the surface of a thin film. This problem is motivated by an interest in the interaction between inhaled droplets and the lungs' thin liquid lining, and the transport of materials contained in the droplet. In the lower respiratory system, the airways and alveoli are covered with a thin liquid lining. Surface-active materials which are believed to be continuously produced by cells lining the alveoli (West 1985; Scarpelli 1988) reduce the surface tension of the air–liquid interfacc and lessen the large external forces that tend to cause alveoli to collapse. A common disease in premature neonates is respiratory distress syndrome which is due to an abnormally high surface tension of the lungs' liquid lining. One possible way to treat this disease is to deliver surfactant exogenously (Enhoring *et al.* 1985; Merritt *et al.* 1986). Substances such as medications or toxins can 'piggyback' onto droplets and reach sensitive regions of the lung (Goetz 1961) by diffusing through a very thin and viscous liquid film. There are a variety of other flows driven

by surface-tension gradients which have applications in engineering. These include coating processes (Ruschak 1985) and crystal growth (Ostrach 1983). For example in coating processes, it is of considerable importance to understand the effects of contaminants (either material or thermal) which can result in non-uniform films.

Borgas & Grotberg (1988), Gaver (1988) and Gaver & Grotberg (1990) investigated the spreading of insoluble surfactant and considered the effects of surface-tension gradients, gravitational forcing and surface diffusivity. They found: (i) that surface-tension-induced convection gives rise to film disturbances that increase the film thickness near the surfactant's leading edge while thinning the film in the central region; (ii) that surface diffusion leads to more rapid spreading and decreases film disturbances; and (iii) that gravity acts as a restoring force by creating bi-directional flow in the form of a ring vortex. We will follow their methods for the corresponding soluble-surfactant problem. The flow field is governed by Stokes equations since inertia terms are small. Furthermore, lubrication theory is used since the film thickness is small compared to the droplet radius. At the interface, there is a coupling between the bulk and surface concentrations of the surfactant that is described by the Langmuir isotherm (Horn & Davis 1975; Probstein 1989). The rigid wall on which the film lies is assumed to be totally permeable to surfactant. This simple condition could be appropriate in cases where surface-active materials are transported through thin films and absorbed by the surrounding tissue before being carried away by the microcirculation. A non-uniform initial surface concentration distribution is chosen, which induces fluid motion and transport within the initially flat film.

In §2, the governing equations for fluid motion and transport are established, and the evolution equations for the film thickness and the surface and bulk concentrations of the surfactant are derived. Results for the time evolution of the film thickness and the surfactant concentration are given in §3. Results concerning the effects of soluble surfactant on transport are presented in §4 and conclusions are given in §5.

2. Governing equations

2.1. *Fluid mechanics of the thin film*

The Stokes flow of a thin liquid layer induced by the axisymmetric spreading of a soluble surface-active material is analysed in this section. As in Gaver & Grotberg (1990), the film is bounded below by a rigid wall at $z^* = 0$ and above by the interface position $z^* = H^*(r^*, t^*)$, such that the axes (r^*, θ, z^*) are fixed at the rigid wall. We apply the lubrication approximations to axisymmetric flow with velocity components $(u^*, 0, w^*)$ since the characteristic lengthscale of the film thickness, H_0, is much smaller than the initial radius of spreading surfactant, R_0. The governing equations are non-dimensionalized by letting

$$\left.\begin{aligned} r^* = R_0 r, \quad z^* = H_0 z, \quad P^* = (S/H_0)p, \quad u^* = u_1 u, \quad w^* = \epsilon u_1 w, \\ \sigma^* = \sigma_m + S\sigma(\Gamma), \quad \Gamma^* = \Gamma_m \Gamma, \quad t^* = (R_0/u_1), \end{aligned}\right\} \tag{2.1}$$

where $\sigma(\Gamma)$ is the surface-tension, a function of the surfactant concentration, $S = \sigma_0 - \sigma_m$ is the spreading parameter, σ_0 is the surface tension of the surfactant-free surface ($\Gamma = 0$) and σ_m is the surface tension of an interface saturated with surfactant ($\Gamma = 1$). The velocity scale, u_1, is obtained by scaling the tangential stress condition at the interface, and is given by $u_1 = \epsilon S/\mu$, where $\epsilon = H_0/R_0 \ll 1$ (Gaver 1988). The reduced momentum equations in the radial and vertical directions are given by

$$\frac{\partial P}{\partial r} = \frac{\partial^2 u}{\partial z^2} + O(\epsilon^2), \quad \frac{\partial P}{\partial z} = -G + O(\epsilon^2), \tag{2.2}$$

where $G = \rho H_0^2 g/S$ is the gravitational parameter. Since the fluid is incompressible, the continuity equation is

$$\frac{1}{r}\frac{\partial}{\partial r}(ru) + \frac{\partial w}{\partial z} = 0. \tag{2.3}$$

The boundary conditions are no slip at the rigid wall

$$u = w = 0 \quad \text{at} \quad z = 0, \tag{2.4}$$

and at the interface we apply the following tangential stress condition:

$$\frac{\partial u}{\partial z} = \frac{\partial \sigma}{\partial r} + O(\epsilon^2), \quad P = O(\epsilon^2) \quad \text{at} \quad z = H. \tag{2.5}$$

Discontinuities in pressure across $z = H$ due to surface-tension forces are $O(\epsilon^2)$ and are therefore neglected.

The momentum equation in the radial direction, (2.2), is integrated twice to yield at leading order

$$u = \frac{\partial P}{\partial r}\left(\frac{1}{2}z^2 - zH\right) + \frac{\partial \sigma}{\partial r} z \tag{2.6}$$

where the pressure, P, is given by

$$P = G(H - z). \tag{2.7}$$

The radial flow rate is defined by

$$Q_r = \int_0^H u \, dz = -\frac{H^3}{3}\frac{\partial P}{\partial r} + \frac{H^2}{2}\frac{\partial \sigma}{\partial r}, \tag{2.8}$$

and conservation of mass then requires that

$$\frac{\partial H}{\partial t} + \frac{1}{r}\frac{\partial}{\partial r}(rQ_r) = 0, \tag{2.9}$$

yielding an evolution equation for the film thickness which is coupled to $\sigma(\Gamma)$.

2.2. *Conservation equations for the surfactant*

Gaver & Grotberg (1990) considered the insoluble-surfactant problem, thus allowing for surfactant to diffuse and be convected along the interface. For the soluble-surfactant case, the surfactant may also diffuse across the air–liquid interface. The concentration in the bulk phase, C, is scaled as follows:

$$C^* = \frac{C_m}{\gamma} C, \tag{2.10}$$

where C_m is the maximum surfactant concentration in the bulk that can exist in equilibrium with the monolayer and γ is a solubility coefficient. On applying the lubrication approximations, the conservation equations at the interface and in the bulk phase are given by

$$\frac{\partial \Gamma}{\partial t} = \frac{1}{Pe_s}\left(\frac{\partial^2 \Gamma}{\partial r^2} + \frac{1}{r}\frac{\partial \Gamma}{\partial r}\right) - \frac{1}{r}\frac{\partial}{\partial r}(ru_s\Gamma) - \frac{\kappa}{Pe_b}\frac{\partial C}{\partial z} + O(\epsilon^2) \quad \text{at} \quad z = H \tag{2.11}$$

and

$$\frac{\partial C}{\partial t} + \frac{u}{r}\frac{\partial}{\partial r}(rC) + w\frac{\partial C}{\partial z} = \frac{1}{Pe_b}\frac{\partial^2 C}{\partial z^2} + O(\epsilon^2), \quad 0 < z < H, \tag{2.12}$$

where u_s is the surface radial velocity, $Pe_s = u_1 R_0/D_s$ and $Pe_b = \epsilon u_1 H_0/D_b$ denote the surface and bulk Péclet numbers, $\kappa = C_m H_0/(\gamma \Gamma_m)$, and D_s and D_b are the surface and bulk molecular diffusivities. The following boundary conditions on C will be considered:

$$C = 0 \quad \text{at} \quad z = 0, \qquad \Gamma = \frac{C}{1+C} \quad \text{at} \quad z+H. \tag{2.13}$$

The first boundary condition implies that the rigid wall is totally permeable. This is relevant to situations where the surfactant is absorbed into the tissue and reaches the nearby microcirculatory system. The second boundary condition, (2.13), describes a coupling between the bulk and surface concentrations of the surfactant (Horn & Davis 1975) which is usually known as the Langmuir adsorption isotherm in reaction kinetics (Walas 1989).

In many pulmonary applications, the bulk Péclet number is much smaller than the surface Péclet number since the molecular diffusivities, D_s and D_b, are of the same order. Therefore, we will assume that $Pe_b \ll 1$ since $Pe_b/Pe_s = \epsilon^2 D_s/D_b$. Then the left-hand side of (2.12) is negligible and the solution for C is linear in z such that

$$C = \frac{\Gamma}{1-\Gamma} \frac{z}{H} \tag{2.14}$$

to leading order. This simplification has the effect of decoupling (2.11) and (2.12), since $\partial C/\partial z$ in (2.11) depends only on Γ and H. In addition, this approximation implies that initially there is surfactant in the bulk phase. This condition could be appropriate in an experimental set-up where a restraining collar containing surfactant is placed in a film, and the surfactant is allowed to equilibrate before the collar is removed (Gaver 1988).

2.3. *The evolution equations*

A system of coupled, nonlinear equations that describe the evolution of the film thickness, H, and the surfactant concentration, Γ, are obtained by combining the conservation equations derived in the previous section. In the small bulk Péclet number limit, equation (2.11) reduces to

$$\frac{\partial \Gamma}{\partial t} = \frac{1}{r}\frac{\partial}{\partial r}\left(r\left[\left(\frac{1}{Pe_s} - \Gamma H \frac{\partial \sigma}{\partial \Gamma}\right)\frac{\partial \Gamma}{\partial r} + \tfrac{1}{2} G \Gamma H^2 \frac{\partial H}{\partial r}\right]\right) - \alpha \frac{\Gamma}{(1-\Gamma)H}, \tag{2.15}$$

where $\alpha = \kappa/Pe_b$ is the solubility parameter. The surfactant is assumed to be highly soluble across the interface ($\gamma \gg 1$), so that α remains finite in the limit $Pe_b \to 0$. Note that the insoluble surfactant case studied by Gaver & Grotberg (1990) is recovered by setting $\alpha = 0$. The kinematic boundary condition, (2.9), yields

$$\frac{\partial H}{\partial t} = \frac{1}{r}\frac{\partial}{\partial r}\left(r\left[\tfrac{1}{3} G H^3 \frac{\partial G}{\partial r} - \tfrac{1}{2} H^2 \frac{\partial \sigma}{\partial \Gamma}\frac{\partial \Gamma}{\partial r}\right]\right), \tag{2.16}$$

where the surface-tension equation of state is the same as that used by Sheludko (1967), Borgas & Grotberg (1988) and Gaver & Grotberg (1990), namely

$$\sigma(\Gamma) = (\beta+1)\,(1+\theta(\beta)\,\Gamma)^{-3} - \beta, \tag{2.17}$$

where $\theta(\beta) = ((\beta+1)/\beta)^{\frac{1}{3}} - 1$, and $\beta = \sigma_m/S$ is the ratio of minimum surface tension to the spreading parameter.

The appropriate boundary conditions on Γ and H are

$$\frac{\partial \Gamma}{\partial r} = \frac{\partial H}{\partial r} = 0 \quad \text{at} \quad r = 0 \tag{2.18}$$

and

$$\Gamma \to 0, H \to 1 \quad \text{as} \quad r \to \infty. \tag{2.19}$$

Initial conditions are also required. The initial surfactant distribution is assumed to be a smoothed disk of surfactant, and is described by the following function:

$$\Gamma(r, 0) = \tfrac{1}{2}\Gamma_{\max}[1 - \tanh(a(r - r_0))], \tag{2.20}$$

where a controls the initial steepness of the surface concentration gradients and r_0 controls the location of the front. Large values of ar_0 are used so that the symmetry conditions at $r = 0$, (2.18), are satisfied within numerical tolerance. $\Gamma_{\max}$ is chosen to be less than 1 so that the solubility term in (2.15) is not singular. The film is assumed to be initially flat:

$$H(r, 0) = 1. \tag{2.21}$$

The stream function was also calculated in order to obtain the streamline patterns for the various flows that will be computed in the next section. Since the flow is axisymmetric, the stream function is given by

$$\psi = -r\left(G\frac{\partial H}{\partial r}(\tfrac{1}{6}z^3 - \tfrac{1}{2}z^2 H) + \tfrac{1}{2}z^2 \frac{\partial \sigma}{\partial \Gamma}\frac{\partial \Gamma}{\partial r}\right) \tag{2.22}$$

where

$$\frac{\partial \psi}{\partial z} = -ru, \quad \frac{\partial \psi}{\partial r} = w. \tag{2.23}$$

3. Results

The system of evolution equations, (2.15)–(2.16), derived in the previous section, are solved numerically for $\Gamma(r, t)$ and $H(r, t)$ using the method of lines (Holt 1984) for a wide range of parameter values and different values of time. The following parameter values which are pertinent to the small airways of the lungs were chosen for illustrative purposes. If $H_0 = 0.001$ cm, $R_0 = 0.01$ cm, $\mu = 5$ cP, $S = 50$ dynes/cm and $D_s = 10^{-4}$ cm^2/s, then $Pe_s = 100$, $G \ll 1$ and one dimensionless time unit is equivalent to 0.01 s. So the surface Péclet number is chosen to be 100, $\alpha = 0.001$, $\beta = 5$, $G = 0$, $a = 10$ and $r_0 = 1$. Gravitational effects can be important in experimental set-ups (Gaver 1988). Figures 1(*a*) and 1(*b*) show the time evolution of the film thickness and the surfactant concentration. In figure 1(*a*), H is plotted as a function r for various times. It shows the propagation of a moving front which initially grows from the uniform state due to large surface-tension gradients (not shown), and then decreases as the gradients become small, with a thinning of the region immediately behind the front. This is consistent with results obtained by Gaver & Grotberg (1990). In figure 1(*b*), the initially steep surfactant gradients disappear as the droplet spreads outward. After a long period of time, $t > 400$, Γ is no longer a monotonically decreasing function of r, but develops a local maximum. This is because H becomes small behind the front and consequently the vertical diffusion gradients become large, taking more mass from the interface. From (2.6) and (2.7) we see that, for $G = 0$, the radial velocity is

$$u = \frac{\partial \sigma}{\partial \Gamma}\frac{\partial \Gamma}{\partial r} z \tag{3.1}$$

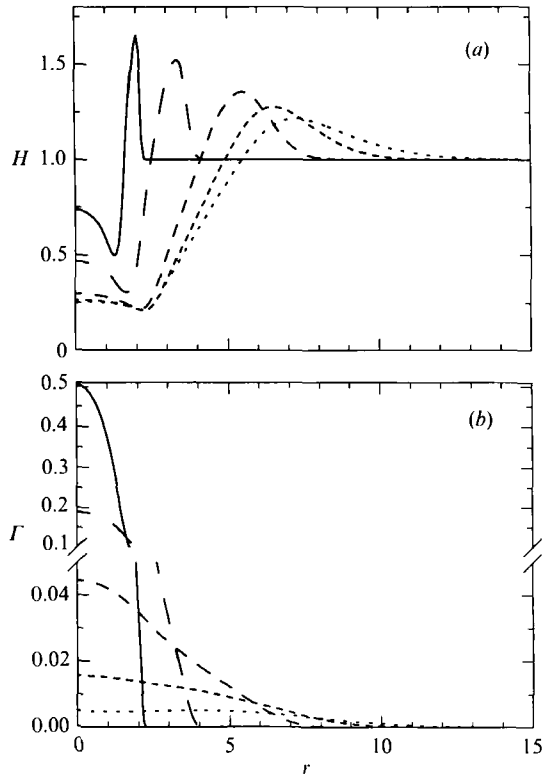

FIGURE 1. (a) Film thickness and (b) surfactant concentration profiles at $t = 200$ (——), 400 (— — —), 600 (– – –), 800 (-·-·) 1000 (·····). $Pe_s = 100$, $\alpha = 0.001$, $\beta = 5$, $G = 0$, $a = 10$ and $r_0 = 1$.

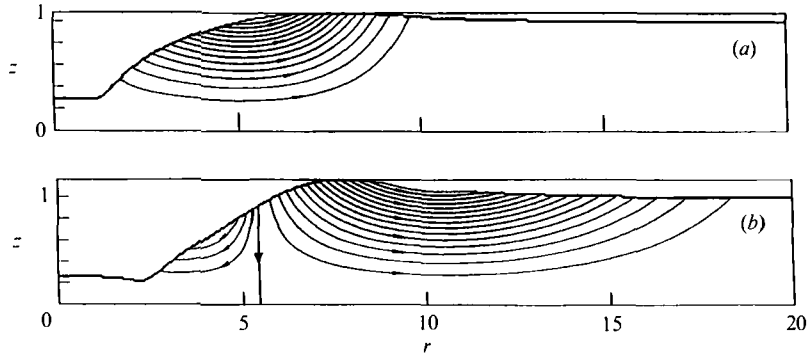

FIGURE 2. Streamline patterns demonstrating the effects of soluble surfactant at (a) $t = 200$, (b) $t = 1000$. $Pe_s = 100$, $\alpha = 0.001$, $\beta = 5$, $G = 0$, $a = 10$ and $r_0 = 1$.

From (2.17), $\partial\sigma/\partial\Gamma < 0$, so (3.1) implies that for all z we expect outward radial flow when $\partial\Gamma/\partial r < 0$ at small t. This behaviour is demonstrated in figure 2(a) which shows the corresponding streamline patterns at $t = 200$. Since figure 1(b) demonstrates an extremum in $\Gamma(r, t)$ for $r > 0$ at large enough t, we can anticipate a division of the flow regime into regions of outflow and backflow (figure 2b). This surface-tension-gradient backflow phenomenon is not observed in the insoluble-surfactant case. In the presence of gravity, $G \neq 0$, there are modifications of this backflow, discussed below, and competition with hydrostatically induced backflow.

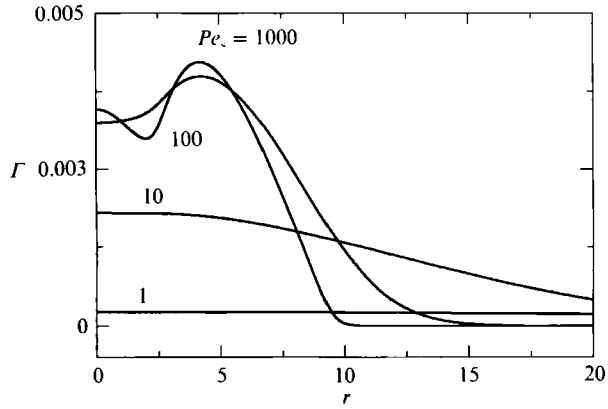

FIGURE 3. Surfactant concentration profiles for $Pe_s = 1, 10, 100, 1000$. $\alpha = 0.001$, $\beta = 5$, $G = 0$, $a = 10$, $r_0 = 1$, and $t = 600$.

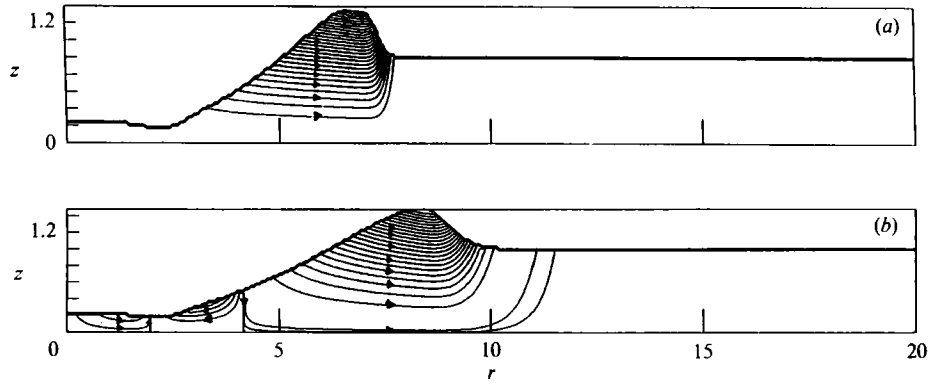

FIGURE 4. Streamline patterns demonstrating the effects of large Pe_s (= 1000) at (*a*) $t = 200$, (*b*) $t = 500$.

The effects of the surface Péclet number are shown in figure 3. The parameter values are identical to those for figure 1 except that Pe_s is allowed to vary. Gaver & Grotberg (1990) showed that increasing Pe_s leads to larger film disturbances. A well demarcated front and a thinning in the region behind it are observed at very large Péclet numbers. As shown in figure 3, the rate of surfactant spreading decreases with increasing Pe_s since this is consistent with decreasing D_s. As in Gaver (1988), analytical solutions for small Pe_s are in good agreement with the numerical results. In the case of $Pe_s = 1000$, a more complicated phenomenon develops. $\Gamma(r, t)$ now has two local extrema for $r > 0$ which will cause the radial convection to have three regimes. This evolution is illustrated in figure 4(*a*, *b*). For small enough time there is only outward flow (figure 4*a*), and for large enough time the pattern divides into two outward flow regions separated by an inward flow region. The local minimum in Γ, near $r = 3$, apparently is related to the local minimum in H, also near $r = 3$.

The influence of the gravitational parameter, G, on the flow field can be seen in figures 5 and 6. The parameter values are identical to those in figure 1 except that G is allowed to vary. We find divisions of radial flow, bounded by streamlines which intersect the surface where $u_s = 0$, as when $G = 0$ above. If G is small enough then the same sort of behaviour as in the case where $G = 0$ and $\alpha \neq 0$ is observed, that is $\partial\Gamma/\partial r$ changes sign resulting in a surface-tension-induced backflow similar to that

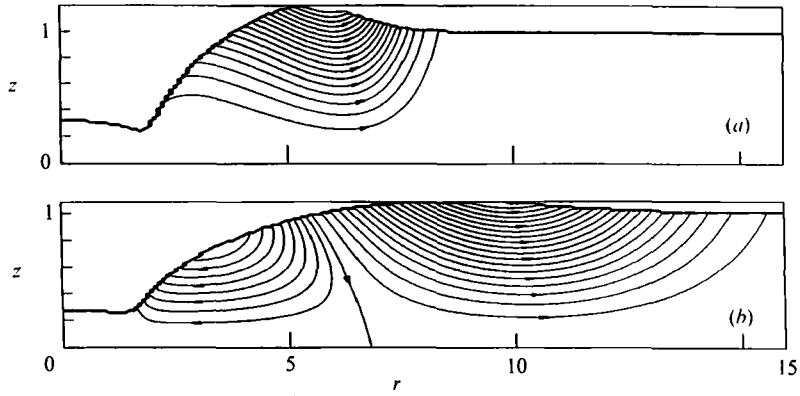

FIGURE 5. Streamline patterns demonstrating the effects of weak gravitational forcing at (a) $t = 70$, (b) $t = 350$. $Pe_s = 100$, $\alpha = 0.001$, $\beta = 5$, and $G = 0.05$.

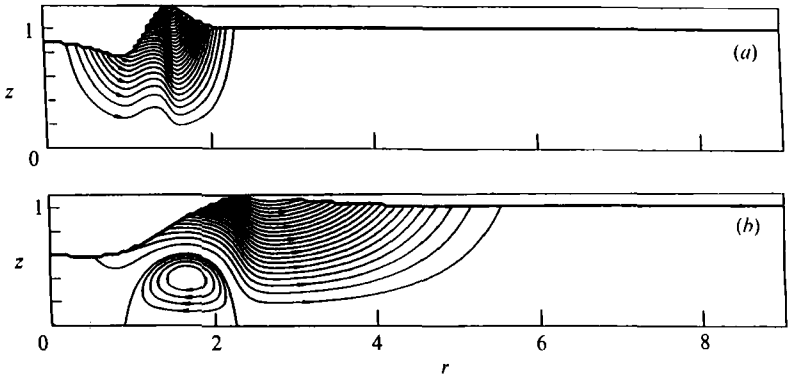

FIGURE 6. Streamline patterns demonstrating the effects of strong gravitational forcing at (a) $t = 0.25$, (b) $t = 3$. $Pe_s = 100$, $\alpha = 0.001$, $\beta = 5$, and $G = 1$.

shown in figure 2. However, since in this case the velocity is a quadratic function of z, (2.6), the dividing streamline between radially outward and backward flow is a curve instead of a vertical line. Streamlines for this case are shown in figure 5(a), (b). If G is large enough the layer does not thin as much and Γ is a monotonic decreasing function of r. Gaver & Grotberg (1990) showed that, in the insoluble case, flow reversal occurs only if gravitational effects are included, since with time, hydrostatic forces become larger than surface-tension gradients. Figures 6(a), (b) shows the streamlines for a case where $G = 1$ and $\alpha = 0.001$ at $t = 0.25$, 3. After a short period of time, the flow is radially outward (figure 6a), but with time a vortex develops at the lower wall (figure 6b) which eventually engulfs the layer behind the moving front. In this case the flow is bi-directional as opposed to the absorption-induced backflow which is observed when G is very small. Flow fields consisting of ring vortices and adsorption-induced backflows are not possible because u is quadratic in z.

4. Transport

In this section we examine the influence of the parameters α, Pe_s, and G on the amount of surfactant being absorbed by the rigid wall and the rate at which surfactant spreads on the thin liquid film. Having some knowledge of the effects of

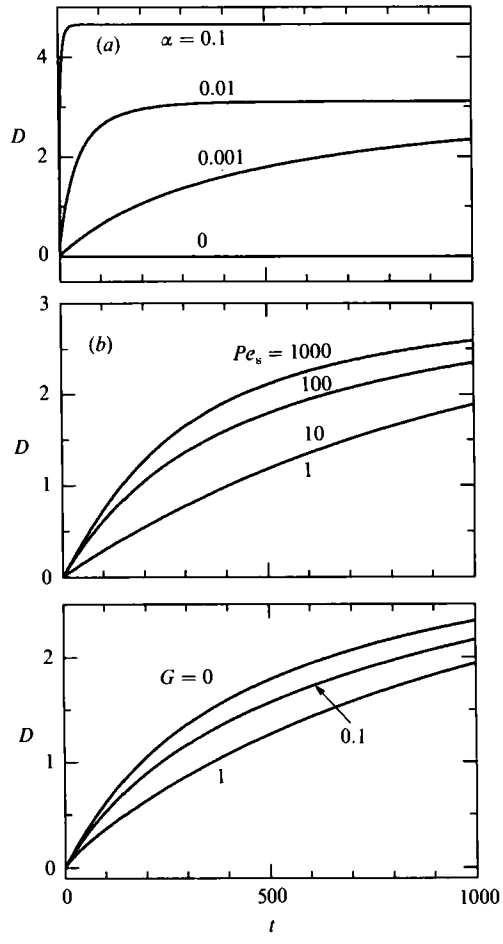

FIGURE 7. Dose versus t. (*a*) $\alpha = 0, 0.001, 0.01, 0.1$, (*b*) $Pe_s = 1, 10, 100, 1000$, (*c*) $G = 0, 0.1, 1$.

solubility, molecular diffusivity and gravity, for example, could be important in certain applications such as drug delivery by aerosol inhalation.

We define the dose, $D(t)$, as

$$D(t) = 2\pi \int_0^t \int_0^\infty (\Gamma(r,0) - \Gamma(r,t))\, r \mathrm{d}r\, \mathrm{d}t, \tag{4.1}$$

Figure 7 (*a*) shows that D increases less rapidly for smaller values of α, as expected. Increasing G slows down the amount of surfactant being delivered (figure 7*c*) since gravity acts as a restoring force thereby decreasing the vertical flux of surfactant across the air–liquid phase. The amount of surfactant delivered is enhanced by increasing Pe_s because of larger film disturbances and the retention of the initially steep gradients at higher Pe_s (figure 7*b*).

One measure of how far the surfactant spreads is given by the droplet radius, R_d. It is defined as follows:

$$R_d = r \quad \text{such that} \quad \Gamma(R_d, t) < \epsilon_d, \tag{4.2}$$

where $\epsilon_d = 10^{-6}$. The effect of α on R_d is shown in figure 8. Increasing α slows down

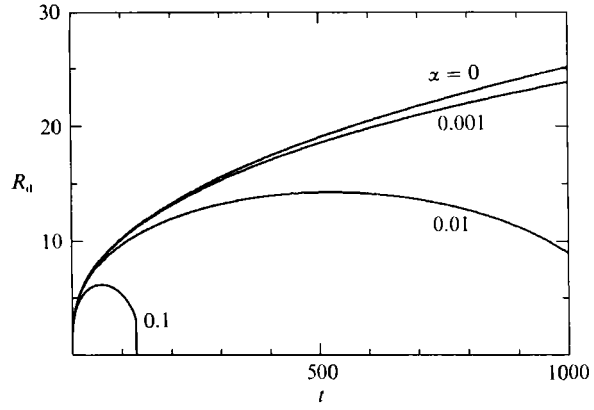

FIGURE 8. Droplet radius versus t. $\alpha = 0, 0.001, 0.01, 0.1$.

the propagation of the concentration front. Eventually, R_d decreases since a backflow is generated for the soluble surfactant cases and drops down to zero when there is no surfactant left on the surface. Another relevant parameter is the position of the convection front, R_c. For fixed $G, R_c > R_d$, which is in agreement with experiments of Gaver & Grotberg (1992). This distinction is caused by the welling of fluid near the droplet's leading edge.

5. Conclusions

We have modelled the spreading of a droplet of soluble surfactant on a thin viscous film driven by surface-tension gradients, surface and bulk diffusion and gravity. The ensuing motion and deformation of the liquid lining play an important role in the transport of dissolved substances from the droplet, through the lining and into the tissue for absorption. The problem considered here represents a starting point for analysing more complex transport models with applications in pulmonary and aerosol dynamics.

Evolution equations describing the variation of surfactant concentration and film thickness were derived using lubrication theory. These could be decoupled from the equation of surfactant concentration in the bulk by taking $Pe_b \ll Pe_s$.

The results of this study demonstrates a strong dependency of the film thickness, surfactant concentration and the dose of surfactant delivered on the surface Péclet number, Pe_s, the gravitational parameter, G, and the solubility parameter, α. As in Gaver & Grotberg (1990), very large film disturbances are obtained at large Pe_s if gravitational effects are neglected, surface diffusion leads to more rapid spreading and smaller disturbances, and gravity also dampens disturbances by creating a bi-directional flow. These can have significant effects on the mass transport of surfactant from the interface into the underlying tissue. As shown in figures 7(*b*) and 7(*c*), the amount of surfactant delivered is enhanced by increasing Pe_s and decreasing G because H becomes small enough that vertical diffusion gradients become large. However, increasing Pe_s decreases the rate at which surfactant spreads and this may be undesirable in certain applications. The dose of surfactant, $D(t)$ saturates very quickly for $\alpha > 0.01$ (figure 7*a*). This may be inefficient if medications in the form of surface-active materials are to reach only the more distal regions of the lower respiratory system.

The solubility parameter, α, also has a strong effect on the flow field and the dose. A backflow can result after a long period of time even for cases where gravitational effects are neglected (figure 2). This is due to a thinning of the liquid layer when $G = 0$ which results in big changes in the bulk-concentration gradients, $\partial C/\partial z$, near the minimum value of $H(r, t)$, and is different from the vortex that develops on the lower wall when gravitational effects are included. For moderate Pe_s and $G = 0$, there is a bounding streamline dividing outward and inward flow, but for sufficiently large Pe_s, as shown in figure 3, a backflow region develops between two outward flow regions since the surface concentration of surfactant develops two extrema.

This research was funded by NIH grants K04-HL01818, R01-HL41126, NSF grant CTS-9013083, as well as a supercomputing grant from the National Center for Supercomputing Applications, University of Illinois, Urbana-Champaign.

REFERENCES

BORGAS, M. S. & GROTBERG, J. B. 1988 Monolayer flow on a thin film. *J. Fluid Mech.* **193**, 151–170.

ENHORING, G., SHENNAN, A., POSSMAYER, F., DUNN, M., CHEN, C. P. & MILLIGAN, J. 1985 Prevention of neonatal distress syndrome by tracheal instillation of surfactant: a randomized clinical trial. *Pediatrics* **76**, 145–153.

GAVER, D. P. 1988 Surfactant-induced soluto-capillary motion by a droplet on a thin film. Ph.D. thesis, Northwestern University.

GAVER, D. P. & GROTBERG, J. B. 1990 The dynamics of a localized-surfactant on a thin film. *J. Fluid Mech.* **213**, 127–148.

GAVER, D. P. & GROTBERG, J. B. 1992 Droplet spreading on a thin viscous film. *J. Fluid Mech.* **235**, 399–414.

GOETZ, A. 1961 On the nature of the synergistic action of aerosols. *Intl J. Air Water Poll.* **4**, 168–184.

HOLT, M. 1984 *Numerical Methods in Fluid Dynamics*. Springer.

HORN, L. W. & DAVIS, S. H. 1975 Apparent surface tension hysteresis of a dynamical system. *J. Colloid Interface Sci.* **51**, 459–475.

MERRITT, T. A., HALLMAN, M. BLOOM, B. T., BERRY, C., BENIRSCHKE, K., SAHN, D., KEY, T., EDWARDS, D., JARVENPAA, A. L., POHJAVUORI, M. 1986 Prophylactic treatment of very premature infants with human surfactant. *N. Engl. J. Med.* **315**, 785–790.

OSTRACH, S. Fluid mechanics in crystal growth. The 1982 Freeman Scholar Lecture. *Trans. ASME* I: *J. Fluids Engng* **105**, 5–20.

PROBSTEIN, R. F. 1989 *Physicochemical Hydrodynamics: An Introduction*. Butterworths.

RUSCHAK, K. J. 1985 Coating flows. *Ann. Rev. Fluid Mech.* **17**, 65–89.

SCARPELLI, E. M. 1988 *Surfactants and the Liquid Lining of the Lung*. The Johns Hopkins University Press.

SHELUDKO, A. 1967 Thin liquid films. *Adv. Colloid Interface Sci.* **1**, 391–464.

WALAS, S. M. 1989 Reaction Kinetics for Engineers. Butterworths.

WEST, J. B. 1990 *Respiratory Physiology – the Essentials*, 4th edn. Baltimore: Williams and Wilkins.